RESEARCH ARTICLE doi.org/10.1002/adsc.202300989 Advanced Synthesis & Catalysis

Very Important Publication

Hydroxamate Assays for High-Throughput Screening of Transketolase Libraries Against Arylated Substrates

Inés Fúster Fernández,[a] Michael Kickstein,[a] and Wolf-Dieter Fessner[a,*]

[a] Institut für Organische Chemie und Biochemie, Technische Universität Darmstadt, Peter-Grünberg-Str. 4, 64287 Darmstadt, Germany
E-mail: fessner@tu-darmstadt.de

Manuscript received: September 5, 2023; Revised manuscript received: October 16, 2023;
Version of record online: November 3, 2023

Supporting information for this article is available on the WWW under https://doi.org/10.1002/adsc.202300989

© 2023 The Authors. Advanced Synthesis & Catalysis published by Wiley-VCH GmbH. This is an open access article under the terms of the Creative Commons Attribution-NonCommercial License, which permits use, distribution and reproduction in any medium, provided the original work is properly cited and is not used for commercial purposes.

Abstract: We recently reported that the transketolase from *Geobacillus stearothermophilus* (TK_{gst}) upon acyl transfer to nitrosoarenes generates *N*-aryl hydroxamic acids (HA). The latter are metal chelating compounds that in the presence of Fe(III) ions form deep-red complexes. Here, we applied this principle to the development of a colorimetric assay in both solid- and liquid-phase formats for the high-throughput screening of TK_{gst} and its variants. Screening a set of positive hits from a L382X/D470X library validated the specificity and sensitivity of the assays. The solid surface assay allows a clear distinction between positive and negative colonies by the naked eye in qualitative mode, and further also to measure activity in semi-quantitative fashion in the liquid-phase format. The assay will be important for engineering the TK_{gst} enzyme towards improved conversion of aromatic aldehydes by their close structural analogy to nitrosoarenes.

Keywords: transketolase; hydroxamic acids; iron (III) chelation; high-throughput screening; colorimetric assay

Introduction

Transketolase (TK, EC 2.2.1.1) is a thiamine diphosphate (ThDP) dependent catalyst that *in vivo* reversibly transfers a hydroxyacetyl moiety from a ketose phosphate to an aldose phosphate in order to connect the pentose phosphate pathway to glycolysis,[1] TK catalyzed reactions lead to a new chiral center with (*S*)-configuration and thereby produce phosphorylated ketoses of D-threo (3*R*,4*R*) configuration. When utilizing hydroxypyruvate (HPA) as the acyl donor substrate, decarboxylation drives the reaction equilibrium towards product formation.[2] The enzyme from *Geobacillus stearothermophilus* (TK_{gst}) has been shown to be a robust catalyst for preparative applications,[3] because of its extended catalyst lifetime at elevated temperatures, improved resistance towards non-conventional reaction media, and significant tolerance to mutagenesis. TK_{gst} has been engineered by *in vitro* evolution for enhanced acceptance of non-phosphorylated sugars,[4] various 2-hydroxyaldehydes,[5] aliphatic[6] and arylated aldehydes,[7] as well as for altered stereoselectivities.[5,8] Also, enzyme variants could be created that are able to utilize various other 2-oxo acids as alternative donor substrates.[9] Although benzaldehyde and a few derivatives have been proven to be acceptor substrates for engineered variants of TK_{gst}[7] and TK from *E. coli*,[10,11] preparative applications suffer from less effective rates and product decay under reaction conditions.[7,10]

We have recently shown that TK_{gst} accepts nitrosobenzene (**1 a**) and variously substituted derivatives as electrophilic substrate components (Scheme 1).[12] When compared to structurally equivalent benzaldehydes, reactivity of nitrosoarenes is significantly enhanced and generates *N*-aryl hydroxamic acids (HA) by carbon-nitrogen bond formation instead of the regular carboligation. HA products readily form metal chelate complexes, which can be used for analytical purposes in case of the deep red color of the iron(III) complex.[12]

© 2023 The Authors. Advanced Synthesis & Catalysis published by Wiley-VCH GmbH

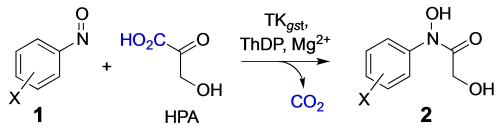

Scheme 1. General TK$_{gst}$-catalyzed reaction of nitrosoarenes with HPA for generation of a carbon-nitrogen bond to yield *N*-aryl HA (**2**).

A critical challenge for projects in directed evolution is the need for a robust, specific, sensitive, and efficient assay method for the high-throughput screening of large libraries of mutants to identify new catalyst variants with novel or improved properties.[13] Several methods for measuring TK activity have been hitherto proposed.[14] Screening for product formation by HLPC[11] or GC analysis[15] is effort- and time-consuming and therefore low throughput. Assays using tetrazolium-based oxidation,[10,11d,16] which are limited to non-hydroxylated aldehyde acceptors, require removal of residual HPA because α-hydroxylated substrates also react with the reagent. Our high-throughput pH-shift assay developed for TK analysis is universal, being independent of substrate structure for both aldehyde acceptor and oxo acid donor moieties.[6,9,14a] Recently, an adaption of this assay has been reported for the screening of TK variants directly on agar plate.[17] However, the pH-shift principle only accounts for the first step in the TK catalytic cycle, *i.e.*, the substrate consumption by decarboxylation, whereas potential hydrolytic decomposition of the cofactor-bound intermediate may indicate false-positive results for the desired second step without giving rise to product formation by carboligation.[11d] The pH assay may also be perturbed by air oxidation of sensitive aldehydes (such as benzaldehyde), which generates acid that is incompatible with the assay principle.

Here, we take advantage of the TK-mediated generation of *N*-aryl HA and demonstrate the application of their complex forming ability with iron (III) ions for the development of a reliable high-throughput assay principle for the colorimetric screening of TK libraries in liquid- or solid-phase formats. This approach makes use of an unequivocal detection of generated product, avoiding the ambiguity from possible false positive hits of the pH-based assay. The iron (III) screening results for the conversion of differently substituted nitrosoarenes are compared to data obtained for conversion of benzaldehyde with the pH-based assay[7] to validate the novel method.

The assay method was first developed and implemented in liquid-phase format in semi-quantitative mode, and then optimized and transferred to a solid-phase supported format to quickly identify active colonies directly from agar plates.

Results and Discussion

Development of a Colorimetric Iron (III) Assay

For the development of a colorimetric assay based on the chelating property of HA towards metal ions, the conditions of its use needed to be considered first. The evaluation of TK activity would have to be determined from assay-volume sized micro-scale conversions of nitrosobenzene derivatives with HPA as substrate donor in the presence of ThDP and Mg^{2+} as cofactors, buffer components, and minor quantities of cell-free extract from protein expression. $FeCl_3$ was chosen to indicate product formation. 1-Bromo-4-nitrosobenzene (**1 b**) was employed as acceptor because of its lower volatility yet similar reactivity in comparison to nitrosobenzene (**1 a**). The TK$_{gst}$ L382 N/D470S variant (short: N/S) was used, which previously was identified for its apparent best reactivity with benzaldehyde (**3**) and preparative utility in the synthesis of *N*-aryl HA.[12]

Standard HA have an extraordinary ability to chelate iron (III) ions. In particular, in alkaline media the dissociable HA with a pK$_a$ of ~9 favors a stable hexacoordinate 3:1 liganded structure.[18] Purified *N*-(4-bromophenyl)-*N*,2-dihydroxy-acetamide (**2 b**) displays an absorbance maximum (λ_{max}) around 500 nm with good stoichiometric linearity.[12]

Interestingly, in orienting tests a disappearance of the HA–Fe(III) complex color was observed upon increasing HPA concentrations (Figure 1).

Apparently, this phenomenon indicates a competing complex formation also between iron (III) and HPA, which seems to form chelates of comparable stability as that with HA. Plausibly, this is due to three alternative chelating motifs for HPA (Scheme 2 A) as compared to the single active HA chelate (Scheme 2 B). In addition, the latter may be electronically

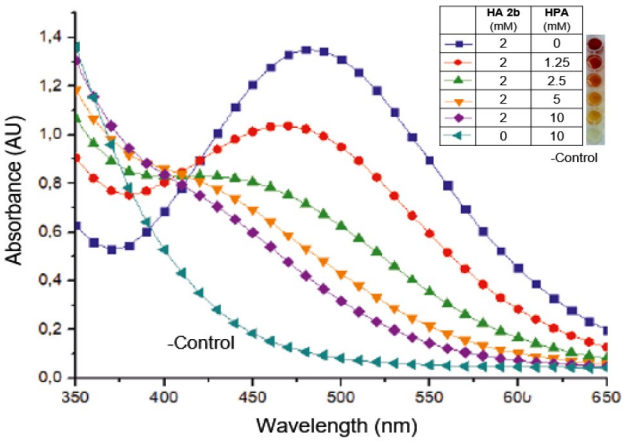

Figure 1. Effect of HPA in HA–Fe(III) complex formation. Conditions: $FeCl_3$ (2 mM), TEA buffer pH 7.45 (2 mM), **2 b** (2 mM) and HPA gradually increasing from 0 to 2 mM.

© 2023 The Authors. Advanced Synthesis & Catalysis published by Wiley-VCH GmbH

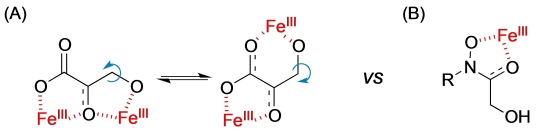

Scheme 2. Plausible chelating positions of Fe(III) with HPA (A) and HA (B).

destabilized by the electron withdrawing α-hydroxyl substituent.

The conflicting interaction of HPA with the essential iron (III) analyte rendered a continuous assay method unreliable, because of its conversion-dependent, varying concentrations. Nonetheless, a discontinuous endpoint assay seemed plausible, where ferric chloride was to be added at a certain time to determine the extent of the enzymatic generation of HA at the expense of HPA reagent (Scheme 3).

Liquid-Phase Screening Assay

For the development of a reliable high-throughput assay, a few critical parameters were optimized initially using pure HPA and HA (**2 b**) in the absence of enzyme. After addition of ferric chloride, pH values dropped to between 2 and 3, which also resulted in a maximum intensity of the red color (Figure S1). Because buffer components may interact with metal ions in a competing manner, five different buffers including phosphate, glycylglycine (Gly-Gly), tris(hydroxy-methyl)-amino-methane (TRIS), 4-(2-hydroxyethyl)-1-piperazine-ethanesulfonic acid (HEPES), and triethanolamine (TEA) were tested at various concentrations from 2 mM to 50 mM (Figure S2). According to this buffer screening, 5 mM TEA was chosen as the optimal buffer. To aid the solubility of the aromatic substrates, DMSO (20%) was chosen as the reaction co-solvent. Acetone had proven superior for the preparative scale synthesis of HA,[12] but was dismissed here because acetone might etch the surface of polysterene microtiter plates and cause unreliable readings over time.

To find the optimal wavelength for the calibration curve for the iron (III) assay, HPA was gradually applied and the amount of HA **2 b** product was varied from 0 to

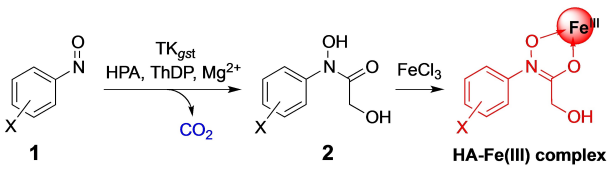

Scheme 3. Principle of the colorimetric Fe(III) assay for evaluation of TK activity in discontinuous fashion. Intermediate **2** is not isolated prior to $FeCl_3$ addition (**2**a: X = 4-H; **2 b**: X = 4-Br; **2 c**: X = 3-CF_3; **2 d**: X = 3-Cl, 4-CH_3).

2 mM (Figure S3). Samples lacking **2 b** were used as negative controls. The calibration curve was then recorded at λ_{max} of 500 nm with variation of the concentration of **2 b** again from 0 to 2 mM (Figure S4). A good linearity was observed, and the limits of detection (LOD) and limits of quantification (LOQ) were derived by linear regression as 0.0154 mM and 0.0466 mM, respectively.

Further aspects were studied such as concentration of substrates and cofactors as well as enzyme quantities. When using clarified cell lysates, the addition of at least 0.6 mM of ThDP and 5 mM of $MgCl_2$ was found to be necessary. The final optimized assay conditions were determined utilizing concentrations of 1.5 mM HPA and 2.0 mM of the corresponding nitrosoarene (**1**).

For a validation of the screening potential of the new assay format, we applied it for testing a selected set of TK_{gst} lysates. Specifically, a microtiter plate was used that contained a collection of 96 positive hits from the L382X/D470X mutant library that were found active against propanal,[6] and also was previously screened against **3**.[7] To test for the anticipated general applicability of the assay, three differently substituted nitrosoarenes with varying constitutional and electronic features were used that had shown good activity in preparative syntheses,[12] namely *p*-bromo- (**1 b**), *m*-(trifluoromethyl)- (**1 c**) and *m*-chloro-*p*-methyl-nitrosobenzene (**1 d**).

Some preliminary tests were run to determine the minimum lysate quantities for reaching sufficient conversion toward HA formation at short incubation times. For **1 c**, the rates of different variants were well discernable with normal lysates, while for **1 b** and **1 d**, the lysates were diluted 1:1 prior to use. Reactions with **1 b** were incubated for 15 minutes at RT, and with **1 c** and **1 d** for 30 minutes. This translates to a relative reactivity of components **1 b**:**1 c**:**1 d** of approximately 4:2:1, which reflects the stereoelectronic effects of their respective substitution patterns. The final colorimetric screening results for the 96-well hit plate of the L382X/D470X library with the selected nitrosobenzene derivatives **1 b–d** under the optimized conditions are shown in Figure 2A–C, respectively, together with sequence information for the individual clones on the plate. On first glance, the color patterns of the three microtiter plates match rather well, reflecting the similar reactivity of the three substrates and indicating high reliability of the assay principle.

The presence of similar protein amounts in each well was confirmed by quantitative analysis of the protein samples using the bicinchoninic acid (BCA) method, which yielded an average of 1740 µg/mL of total soluble protein in the lysate (Figure S7A). Additionally, a selection of eight random samples including both active and inactive variants (A3: I/S; A11: N/S; B1: N/V; C1: L/M; C9: D/S; F2: D/G; H2: D/V; H7: L/T) were compared against a sample of the purified TK_{gst} N/

© 2023 The Authors. Advanced Synthesis & Catalysis published by Wiley-VCH GmbH

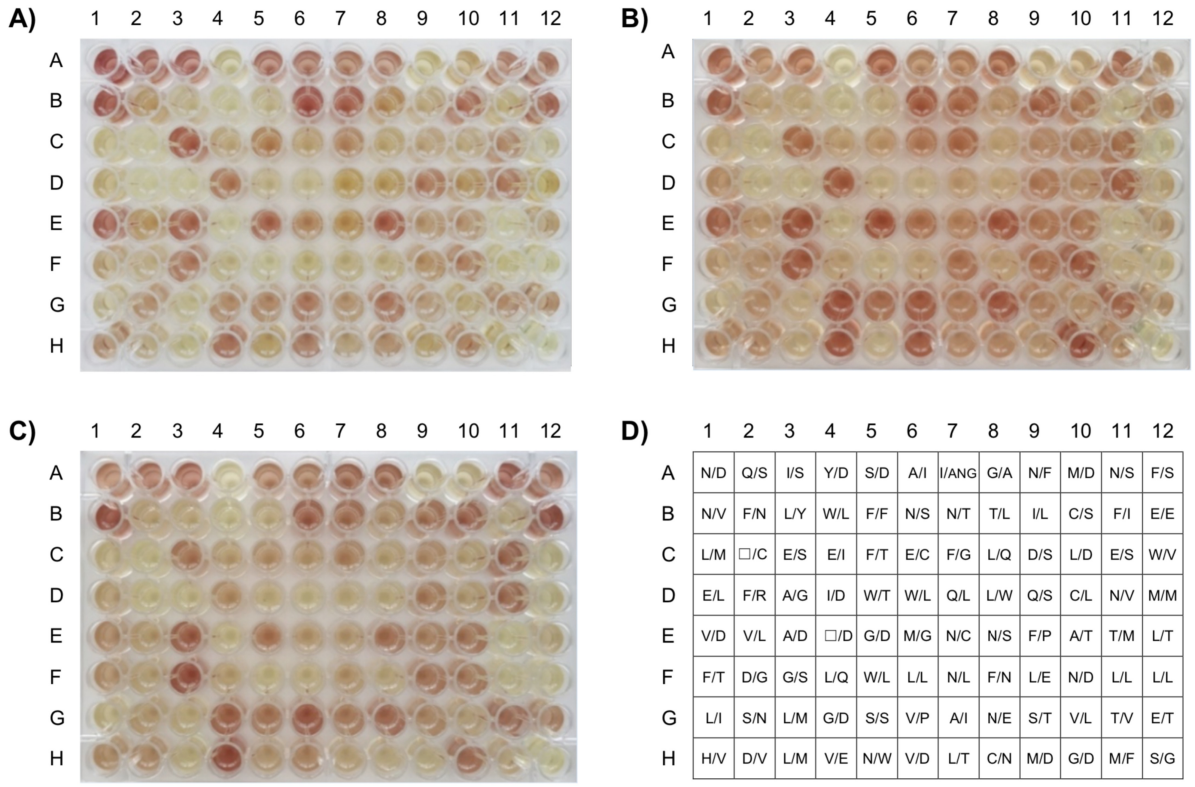

	1	2	3	4	5	6	7	8	9	10	11	12
A	N/D	Q/S	I/S	Y/D	S/D	A/I	I/ANG	G/A	N/F	M/D	N/S	F/S
B	N/V	F/N	L/Y	W/L	F/F	N/S	N/T	T/L	I/L	C/S	F/I	E/E
C	L/M	□/C	E/S	E/I	F/T	E/C	F/G	L/Q	D/S	L/D	E/S	W/V
D	E/L	F/R	A/G	I/D	W/T	W/L	Q/L	L/W	Q/S	C/L	N/V	M/M
E	V/D	V/L	A/D	□/D	G/D	M/G	N/C	N/S	F/P	A/T	T/M	L/T
F	F/T	D/G	G/S	L/Q	W/L	L/L	N/L	F/N	L/E	N/D	L/L	L/L
G	L/I	S/N	L/M	G/D	S/S	V/P	A/I	N/E	S/T	V/L	T/V	E/T
H	H/V	D/V	L/M	V/E	N/W	V/D	L/T	C/N	M/D	G/D	M/F	S/G

Figure 2. Color screening results with the three nitrosoarenes; A) **1 b**, B) **1 c**, C) **1 d**. For A and C, the lysates were diluted 1:1 prior to use. Plate A was incubated for 15 min, and plates B and C for 30 min at RT. Corresponding mutations from the L382X/D470X library are shown in a one letter code mode. □: Stop codon; ANG: A + overlapped peaks (ATGC) + G.

S variant by density measurement of an SDS-PAGE analysis (Figure S7B). Accordingly, around 84% of the lysates consisted of the desired TK protein (Figure S8).

On closer inspection of the numerical screening data, which were averaged from duplicate experiments and normalized (Figure 3A–C), the assay results proved to be consistent as evident from data for some variants that were present as duplicates or even triplicates in the plate. For example, all wells containing the N/S (A11, B6, E8), E/S (C3, C11), G/D (E4, H10), or N/V (B1, D11) genotypes showed similar levels of activity, and also all wells containing the L/L (F6, F11, F12), or L/M (G3, H3) genotype showed no activity.

To evaluate the suitability of the final ferric chloride assay for library screening, the statistical *Z*-factor was calculated for the three nitrosoarenes as $Z = 0.76$ for **1 b**, $Z = 0.88$ for **1 c**, and $Z = 0.82$ for **1 d**. In all three cases, these *Z*-factors indicate excellent suitability of the colorimetric assay for high-throughput screening of TK_{gst} libraries with nitrosoarenes.

Interpretation of Assay Results with Identified Hits

Residue Asp 470 is responsible for the control of enantioselective binding of (2*R*)-configured hydroxyaldehydes by specific hydrogen bond formation,[19] whereas Leu 382 is located at the opposite wall of the substrate binding channel and providing a hydrophobic contact. Therefore, the TK_{gst} L382X/D470X library had been created in a two-pronged effort for either improving conversion of simple aliphatic substrates,[6] or changing enantiomer selectivity for 2-hydroxyaldehydes by offering a transposed hydrogen bonding pattern.[6] For example, non-polar replacements D470I or D470 L significantly improved the binding of aliphatic aldehydes, while variants with an inverse L382D polarity showed good reactivity with (2*S*)-configured hydroxyaldehyde antipodes.[5]

Whereas the wild-type TK_{gst} showed almost no conversion with benzaldehyde (**3**), variant L382 N/D470S had been identified for good synthesis activity.[12] Apparently, replacement of the bulky L382 by a smaller residue and of the negatively charged D470 for polar but uncharged Ser (or Thr) residue seemed to improve the productive binding of the sterically demanding arene unit. In line with their close structural similarity to **3**, the nitrosoarenes **1 b–d** elicited a similar activity pattern (Figure 2). No or hardly any activity was observed for variants containing the native L382 residue, such as in combinations with D470X (X=I, L, M, Q, T, W or Y), with the exception of the L/E (F9) variant. Wild-type TK_{gst} (C10) was also essentially inactive. Likewise,

© 2023 The Authors. Advanced Synthesis & Catalysis published by Wiley-VCH GmbH

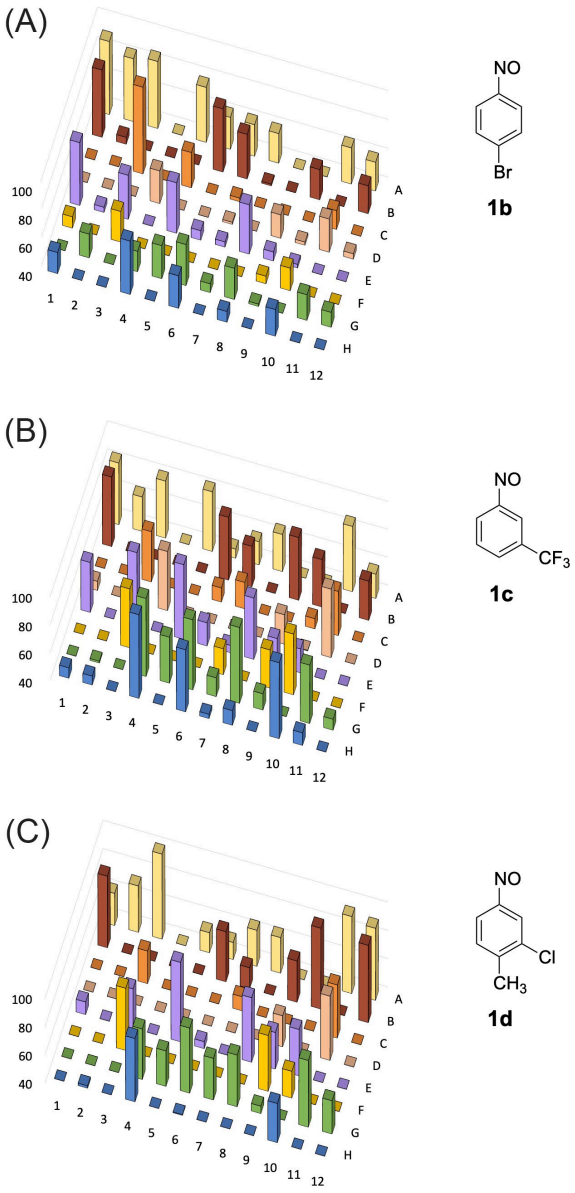

Figure 3. Absorbance screening results from the Fe(III) assay with the three nitrosoarenes **1 b** (A), **1 c** (B), **1 d** (C). Data represent the average of duplicate measurements.

bulky W/X, Y/X and F/X combinations were inactive with the exception of F/S (A12) and F/G (C7) variants that displayed some conversion. Interestingly, a few variants having a bulky but more flexible Ile or Met residue in position 382, such as I/D (D4), I/S (A3) or M/G, were active.

In comparison, allowed modifications of the D470 position seemed to be rather conservative, as most of the 34 clones showing medium to high activity contained either Asp or Ser (65%). Some others also included Thr or Glu as similar hydrogen-bonding residues, plausibly required to activate the electrophilic substrate (aldehyde carbonyl or nitroso group) by protonation.

The comparison of data for the top active variants revealed that three genotypes G/D (E5), N/V (B1) and V/E (H4) showed high conversion (≥75% of the maximum) with all three individual substrates, qualifying them as all-round catalysts for this class of test compounds. The second best group was made up of four genotypes A/D (E3), I/S (A3), N/S (A11, B6, E8) and V/P (G6), which showed a similarly high conversion level only with two of the substrates.

For the bond-forming step, a nitrosoarene must enter the active site head-on, while the *m*- or *p*-positioned substituents in **1 b–d** will point outward and are not expected to contact the mutated residues. While the substituents are electronically different from each other, their steric requirements are relatively similar. Yet, relative activities of some variants were found to be quite different. For example, N/D (A1) and V/D (E1) had high, medium and low activity with **1 b**, **1 c**, and **1 d**, respectively; an opposite behaviour was observed for I/L (B9) and L/E (F9), which had barely any, medium and high activity with this set. In the absence of a reliable structural binding model, such significant catalytic rate differences for the various substrates may be interpreted as due to a distinct electron distribution in the nitrosoarene cores and resulting polarity patterns rather than stemming from steric effects. This observation underscores the usefulness of the HA assay for protein engineering purposes.

Comparison to pH-Shift Screening of Benzaldehyde

Previously, we showed that TK_{gst} is able to accept nitrosoarenes (**1**) as an alternative electrophilic substrate, probably because of its high structural similarity to benzaldehyde (**3**) (Scheme 4).[12] Thus, in order to further validate the colorimetric assay results, data obtained for the TK_{gst} library with the different nitrosoarenes (**1 b–c**) were compared to the results previously obtained for conversion of the structurally equivalent benzaldehyde (**3**) with HPA by using the pH-shift assay

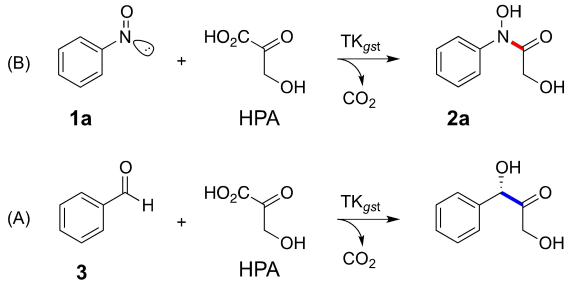

Scheme 4. Comparison of the general TK_{gst} catalyzed reaction of (A) nitrosobenzene **1 a** *versus* (B) benzaldehyde **3** in the presence of HPA.

© 2023 The Authors. Advanced Synthesis & Catalysis published by Wiley-VCH GmbH

(Figure 4).[7] The screening results presented some ambiguity, although the best candidates identified as positive (e.g., N/S) could subsequently be verified by preparative synthesis reactions.

When compared to the nitrosarene screening, the pH data do not match well, because this screening method has a significantly lower confidence interval. Problems arise due to several factors: (i) benzaldehyde is a less reactive electrophile due to resonance effects, which requires longer observation periods; (ii) unavoidable air oxidation of benzaldehyde yields benzoic acid, which causes the pH to decrease continuously and diminishes the assay response; (iii) some active catalysts solvolytically decompose the ThDP bound acyl fragment (formed upon HPA decarboxylation) to liberate glycolaldehyde and thereby cause false positive results (Figure 5), because the released glycolaldehyde is a much better substrate than benzaldehyde.[2b,20] This feature is particularly strong with those D470(S/T) variants, where L382 has been replaced by Asp or Glu (*e.g.*, D/S, C9; E/S, C3, C11; and E/T, G12), but to a lesser degree also evident for Asn (*e.g.*, N/S, A11, B6, E8). For this reason, background correction is essential.

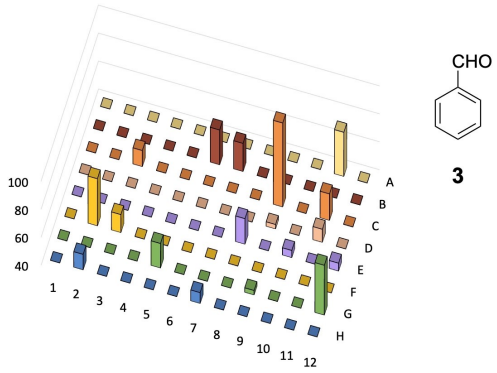

Figure 4. Screening results with benzaldehyde and HPA using the pH-shift assay with phenol red as indicator. Data represent the average of duplicate measurements.[7]

Asn replacement at the L382 position appeared to be one of the best tolerated variations for TK_{gst} with nitrosoarenes, and when combined with a well-tolerated serine, a very active N/S candidate is produced (A11, B6, E8). Indeed, with **3** this also was one of the most active candidates among the positive hit plates from the L382X/D470X library.[7] Although consistent data are obtained with the nitrosoarene assay that prove successful catalysis for ligation, potential acyl hydrolysis (and concomitant loss of HPA) remains unnoticed. Therefore, only a combination of data from the pH-shift assay (i.e., negative control without electrophile) allows eliminating those candidates that are productive but less efficient due to partial substrate decomposition. Even the N/S variant, which has proven synthetic activity with **3**, also shows some activity with the pH assay in the absence of aldehyde.

Nevertheless, from a combined evaluation it appears that a number of variants with good synthetic activity for HA formation seem to retain a stable acyl-ThDP intermediate, these are characterized by an unchanged

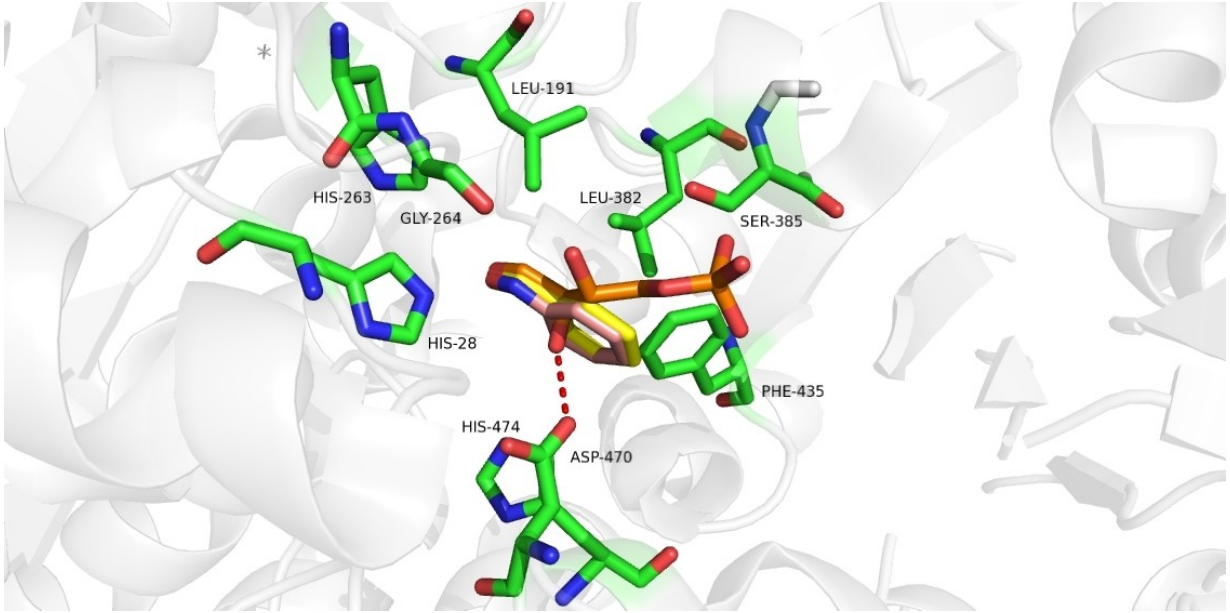

Figure 5. Model of the acceptor-binding pocket employing the X-ray crystal structure of TK_{ban} (PDB entry 3 M49) with substrate conformation of E4P (orange) from the TK_{yst} crystal structure (PDB entry 1NGS). The dotted red line corresponds to a hydrogen bond interaction. Benzaldehyde (**3**, yellow) and nitrosobenzene (**1 a**, salmon) are superimposed to match the carbonyl moiety of E4P. Residue numbering corresponds to TK_{gst}. Image generated with PyMOL.[21]

© 2023 The Authors. Advanced Synthesis & Catalysis published by Wiley-VCH GmbH

D470 residue in combination with a L382X replacement by a smaller residue (X=G, A, S, V; less for N, I); even the constitution V/E or E/E fall into this group. This finding is a bit surprising, because the anionic D470 (or D470E) by its location should be positioned in direct contact with the large hydrophobic aromatic system (Figure 5).[7] These newly identified variants, upon verification by preparative synthesis with benzaldehyde (**3**), are plausible starting points for further engineering of improved TK_{gst} catalyst.

Because the structures **3** and **1** are extremely similar, the strong experimental rate differences must be due to electronic factors favoring the nitroso moiety, particularly in the second, ligation phase of the TK catalysis. Replacement of the carbonyl group for a nitroso group could give an opportunity for **1 a** not only to form polar substrate-enzyme interactions through its oxygen, as with **3**, but also potentially through its lone electron pair at the nitrogen atom, what would improve the TK acceptance for **1** over **3**. To confirm and better understand the difference in TK activity with **1** and **3**, further targeted mutations at related positions would be needed to investigate this further.[8,22] However, it remains difficult to draw conclusions in the absence of an accurate substrate-binding model for such aromatic substrates.

Solid-Supported Screening Assay

Screening assays to identify enzyme candidates of interest[23] may be conducted at various levels of miniaturization with intact cells or with lysates, and coarsely subdivided into two main types: assays on solid-phase or in liquid-phase.[24] Liquid-phase screening methods have been most extensively used because they allow the detection of even small improvements in the desired enzyme property, which is difficult with screening methods on agar plates.[25] However, liquid-phase assays are quite demanding in time, effort and material consumption when screening large directed evolution libraries due to the need for many sample handling steps such as colony picking, protein expression, cell lysis, centrifugation, and liquid transfers. Therefore, solid-phase supported assays on a colony level are an alluring alternative, because they are rapid, efficient, economic and easy to handle. However, the pH-shift method recently reported by the Hecquet group[17] is unreliable for the target of this study because the high volatility of nitrosobenzene and the oxygen sensitivity of benzaldehyde both compromise the readings. The unique product detection strategy using the colorimetric iron (III) assay was therefore highly attractive to be transferred to a solid-phase support, allowing screening assays directly on agar plates and thereby avoiding the extraction of enzymes and the need for specialized equipment.

To prove the feasibility of this method, first practical tests were performed with *E. coli* BL21(DE3) cells expressing the TK_{gst} N/S variant as a positive control and the untransformed BL21(DE3) host strain as a negative control. After growth of recombinant *E. coli* cells on agar plates overnight, colonies were first transferred to a nylon membrane and protein expressed. Permeabilization of the cells by immersion in liquid nitrogen was found to be key for the assay to be successful (Supporting Information page S11). The membrane was placed on top of a filter paper soaked in a reagent solution and incubated for half an hour. Finally, the membrane was dipped into an aqueous $FeCl_3$ solution for color development and hit identification. The general experimental procedure for the colony-based iron (III) assay on agar plate is depicted in Scheme 5.

In comparison to the liquid-phase iron (III) assay conditions had to be adapted and optimized to offer a rapid, reliable and sensitive solid-phase supported screening method. First of all, nitrosobenzene (**1 a**) was employed as acceptor for the solid-phase method instead of **1 b**, because the former can be obtained commercially at acceptable price and purity ($\geq$ 97%), and also because its solubility in water is significantly higher. Addition of TK cofactors (0.6 mM ThDP, 2.5 mM $MgCl_2$) was found crucial for reproducible color differentiation (Supporting Information page S11). From tests with various concentrations of HPA and **1 a** (5–15 mM), the higher concentrations gave the best distinction between positive and negative colonies against background coloration (Supporting Information page S11).

The $FeCl_3$ concentration had to be drastically increased to around 250 mM because lower concentrations in the range of the liquid-phase assay (2–12 mM) did not induce color formation. Dipping the membrane was giving a better homogeneity than

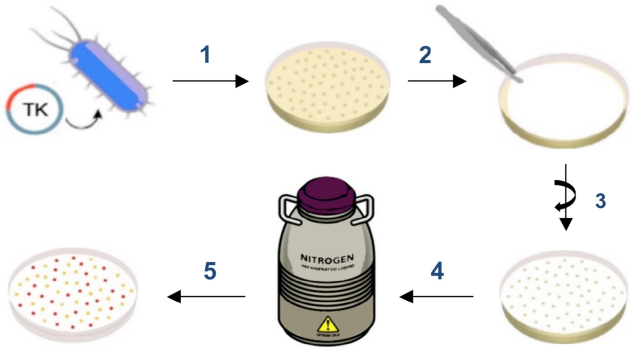

Scheme 5. General procedure of solid-phase supported screening assay with Fe(III). Steps 1) *E. coli* transformation with plasmid and colony growth on LB agar plate; 2) transfer of colonies onto nylon Hybond-N-membrane; 3) protein expression on induction plate; 4) cell permeabilization by immersion in liquid nitrogen; 5) incubation with reagents and subsequent immersion in aqueous $FeCl_3$ solution for screening of active variants.

© 2023 The Authors. Advanced Synthesis & Catalysis published by Wiley-VCH GmbH

spraying with the $FeCl_3$ reagent. Substrate incubation for only 30 minutes was found to give good color differentiation.

The colonies expressing the variant TK_{gst} (N/S) turned red upon contact with $FeCl_3$, in some cases with a violet halo surrounding the colonies, but no coloration was observed for colonies containing the TK_{gst} empty plasmid, allowing a good signal-to-noise ratio for the differentiation of active *versus* inactive colonies. No red color formation (nor violet halo) was observed in the absence of substrates as negative control, neither for the colonies expressing the N/S variant nor for the negative control (Supporting Information page S12).

These initial tests allowed us to check the sensitivity and specificity of the solid-phase assay. To demonstrate the usefulness of the optimized iron (III) based assay as a primary screening tool for the evaluation of TK_{gst} variant libraries on agar plate, the method was applied to the screening of an artificial library generated by mixing all 96 variants contained in the microtiter plate (Figure 2). By using this specific collection of clones with known genetic variety, a direct comparison to results obtained with the previous screening in the liquid-phase was possible. Indeed, the assay resulted in diverse intensities of coloration, ranging from yellow to dark red depending on the activity of the individual colonies carrying the specific mutations (Figures 6A; S14). The most active colonies could be easily identified with excellent contrast because they turned dark red upon contact with the $FeCl_3$ solution, whereas the inactive colonies only became faintly yellow or orange. No red coloration was observed for the same plate in the absence of TK substrates as a negative control (Figure 6B).

To confirm the visual assay results, a random set of colored colonies, including six red (1–6) and three yellow colonies (7–9), was picked from the corresponding master plate and sequenced (Figure S15). The results were in full agreement with the liquid-phase screening data, as all the positive hits (red) had shown activity with all substrates (1: S/D; 2: E/S; 3,4: Q/S; 5,6: N/S), while for the yellow clones no activity had been recorded (7: S/G; 8: Y/D; 9: STOP codon; Figure S16). The consistency of the results between the solid- and liquid-phase assays validates the iron (III) assay as an efficient, sensitive and rapid screening method.

Two shortcomings must be noted that may affect a routine implementation of the colorimetric solid-phase supported assay: 1) The cells are no longer alive after the assay treatment and must be picked from the corresponding colonies on the master plate; 2) the color of colonies may disappear fairly fast and result in a purplish halo in the membrane. This phenomenon is likely due to the diffusion of the HA–Fe(III) complex and may complicate the direct identification of hits from the membrane at extended times (Figure S27). Nevertheless, these limitations can be circumvented by recording an image of the assayed membrane directly after color development for a comparison to the master plate. Thus, colonies do not have to be picked immediately, facilitating the simultaneous treatment of multiple membranes, and the images can be processed electronically for improved colony discrimination. It should be pointed out that during the process no dialysis step was required to remove unspecific background noise, which renders the ferric chloride assay significantly faster than related solid-phase assays.[17,26]

Overall, our novel colorimetric agar plate screening method has the potential to accelerate the throughput for hit identification by at least one order of magnitude in comparison to liquid-phase methods, while simultaneously reducing both handling effort and assay costs. The same assay principle thus allows rapid hit identification on solid support and subsequent characterization in liquid-phase by quantitative microtiter plate assay (Scheme 6).

Conclusion

In this proof-of-principle study, we have developed a novel, highly sensitive colorimetric assay method that

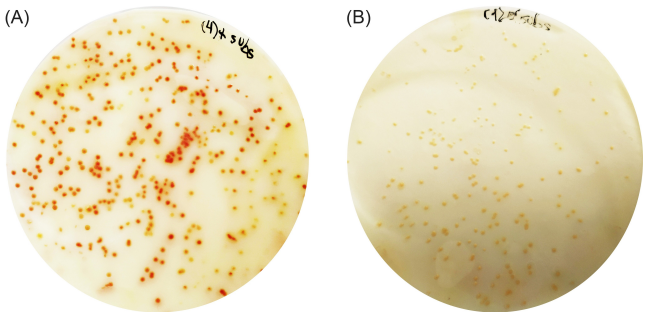

Figure 6. Screening results with the solid-phase Fe(III) assay, A) in the presence, B) in the absence of substrates.

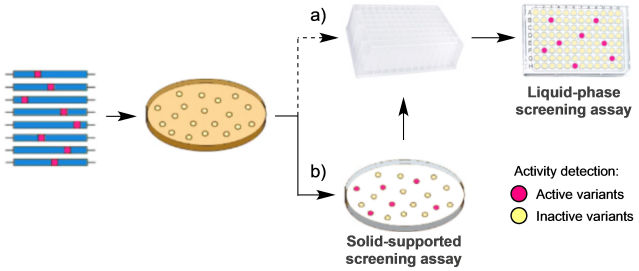

Scheme 6. General workflow of a colorimetric Fe(III) screening using a mutant library grown as colonies on agar plate. a) Conventionally, all colonies are harvested, mutated enzymes expressed and liquid phase-screening is conducted; b) colonies are directly screened for active variants in a solid-surface screening assay, followed by characterization of active hits only in liquid phase.

© 2023 The Authors. Advanced Synthesis & Catalysis published by Wiley-VCH GmbH

can be applied for high-throughput screening and substrate profiling of TK activity. The assay is based on the TK catalyzed conversion of nitrosoarene substrates with specific formation of *N*-aryl hydroxamic acids, which develop a deep red colored chelation complex in the presence of $FeCl_3$, thus allowing a direct readout without the need for auxiliary enzymes. The assay principle could be successfully optimized as an endpoint assay for microtiter plate screening in liquid-phase or alternatively on solid support for direct colony screening. However, the continuous colorimetric monitoring of conversion for kinetic purposes was not possible due to a strong competing chelation of iron (III) ions by the co-substrate HPA.

The liquid-phase assay was validated by screening a microtiter plate containing a collection of hits from the TK_{gst} L382X/D470X library[6] using three structurally different nitrosoarenes as electrophilic substrates. The assay showed high sensitivity and reproducibility, and excellent suitability as a high-throughput screening tool according to the statistical *Z*-factors.

The screening of the library with nitrosobenzene, yielded the same hits that had been identified earlier with the structurally closely related benzaldehyde by using the pH-shift assay, but further revealed a much larger number of active variants having this novel specificity. Because the Fe(III) assay unambiguously detects product formation rather than only substrate decarboxylation, and because the signal can be measured with much higher sensitivity and reliability, the value of screening data generated by the new method is far superior. However, identification of positive hits that are devoid of decomposition of the acyl-ThDP intermediate will require an independent test, either by using the pH assay or determination of erythrulose formation in case of HPA as the nucleophile source.

The Fe(III) colorimetric assay principle could be further developed for colony screening on agar plates, which allows the *in situ* detection of active TK_{gst} variants with the naked eye from larger enzyme libraries. This facilitates the fast identification of hits and so reduces the screening effort in directed evolution by selecting only active clones for subsequent characterization. The screening method was validated by using an artificial library made up from the same collection of candidates from the TK_{gst} L382X/D470X library, which confirmed that both assay methods are consistent, sensitive and reliable for giving reproducible results. Particularly, the cheap and easy agar plate assay should accelerate primary screening by at least one or two orders of magnitude as compared to the liquid-phase method, while being more economical.

We anticipate that the method should prove especially valuable for the identification of enzyme variants from libraries designed for increasing the nucleophile scope against a standard nitrosobenzene electrophile, where less or no competition for complex formation is to be expected than found with HPA. It also should be applicable for evolving TK enzymes with a wider specificity for aromatic substrates by using nitrosoarenes carrying various functionalities in the arene ring. More generally, the assay principle could be adapted for studying other ThDP dependent enzymes involved in the metabolic conversion of nitrosoarenes.[27]

Experimental Section

Materials and Methods

Commercial solvents and reagents were purchased from global vendors and used without further purification. HPA was synthesized as the lithium salt according to a literature procedure.[28] The *E. coli* BL21 (DE3) strain was obtained from New England BioLabs. 96-Well microtiter plates and the acetate film to cover them were acquired from Sarstedt. Incubation was performed in a Heidolph Titramax incubator 1000 model. The autoclave was from Systec VX 150. The hybond-N-Membrane (0.45 µm RPN.303 N) was obtained from Amersham and the filter paper (90 mm) from Macherey-Nagel. Analytical TLC was performed on Merck silica gel plates 60 GF254 using *p*-anisaldehyde stain or iron (III) chloride stain for detection.

Standard Operating Procedure (SOP) for Protein Expression for Library Screening

To a round bottom microtiter plate, LB medium (130 µL) containing kanamycin (50 mg/mL) was added. The plate was covered with a sealing foil and a hole was perforated in each well for aeration. Meanwhile, the glycerol stocks from the library plate were thawed at room temperature. The foil was shortly removed to inoculate the prepared plate with 5 µL of each clone, the plate was sealed again and incubated at 37 °C and 900 rpm for 8 hours. The resulting pre-cultures (100 µL) were transferred to a 96-deepwell plate filled with LB medium (400 µL, containing 50 mg/mL of kanamycin and 0.1 mM IPTG), and the plate was sealed, perforated and incubated at 30 °C and 1200 rpm overnight ($OD_{600} < 0.6$). After incubation, the deep-well plate was centrifuged at 4000 *g* for 20 min at 4 °C. The culture medium was removed, the pellet resuspended with TEA buffer (200 µL, 5 mM, pH 7.45), and the plate centrifuged at 4000 *g* for 20 min at 4 °C. The supernatant was discarded again and the pellets were frozen at −80 °C. For screening, the frozen pellets were thawed and resuspended in lysis buffer (200 µL, TEA buffer (5 mM, pH 7.45), 0.5 mg/mL lysozyme and 4 U/mL cyanase). The deep-well plate was sealed and incubated at 37 °C for 1 hour, followed by 30 min at 50 °C for heat-shock purification. The plate was allowed to stand at room temperature for 15 min for the settlement of the precipitated proteins, and then centrifuged at 4000 *g* for 30 min. The resulting supernatants were transferred to 96-well flat bottom plates for assay measurements.

Final Conditions for the Liquid-Phase Assay with the TK_{gst} L382X/D470X Library

The substrates **1 b**, **1 c**, and **1 d** were screened with the endpoint assay using cell-free lysates as the reaction catalyst. Directly

© 2023 The Authors. Advanced Synthesis & Catalysis published by Wiley-VCH GmbH

after lysis, the resulting supernatants (20 µL) were transferred to 96-well flat bottom plates. For the substrates **1 b** and **1 d** the lysates were diluted 1:1 prior to use. To the 96-well plates, $MgCl_2$ (5 mM), ThDP (0.6 mM), TEA buffer (5 mM, pH 7.45) and HPA (1.5 mM) were added. The reactions were initiated by the addition of the corresponding nitrosoarene (40 µL, 2 mM) dissolved in aq. DMSO (20%). The total volume in each well was 200 µL. The reactions were incubated at RT and 900 rpm for 30 min in the case of the substrates **1 c** and **1 d**, and for 15 min for **1 b**. After the corresponding incubation time, aq. $FeCl_3$ (5 µL, 6 mM) was added, and the solutions were mixed by short vortexing. The absorbance values were read by plate-reader at 500 nm. The absorbance results were treated, normalized and converted to graphical representations. The raw and treated data are found in the Supporting Information (page S5–8).

Calibration Curve, Limit of Detection and Limit of Quantification

To generate a calibration curve for the ferric chloride assay, a series of gradually increasing final concentrations of **2 b** dissolved in methanol from 0 mM to 2 mM in a 96-microwell flat plate were utilized. Simultaneously, gradually decreasing final concentrations of HPA and **1 b**, dissolved in TEA buffer (5 mM, pH 7.45) and methanol respectively, both from 2 mM to 0 mM were applied. The reactions also contained extra volume of TEA buffer (5 mM, pH 7.45) and $FeCl_3$ (6 mM). The total volume was 200 µL. Experiments containing the same amount of TEA buffer (5 mM, pH 7.45), $FeCl_3$ (6 mM), and methanol where corresponding, yet no substrates or HA product, were prepared as controls. The absorbance of the solutions was measured at 500 nm by plate reader and a standard curve $\boldsymbol{y = ax + b}$ was obtained. LOD was calculated as $\boldsymbol{LOD = 3.3Sb/\bar{a}}$, and LOQ was defined as $\boldsymbol{LOD = 10Sb/\bar{a}}$, where *Sb* is the standard deviation of the control.

Z-Factor Calculation

For the evaluation and validation of the liquid-assay method, the *Z*-factor was calculated separately using the data of the assays with the three substrates **1 b**, **1 c** and **1 d** according to the formula

$Z = 1-[(3\cdot(\sigma s+\sigma c))/|\mu s+\mu c|]$, where σs is the standard deviation of the sample, σc is the standard deviation of the control, μs is the sample average, and μc is the control average. The assay method is judged to be ideal when $Z = 1$, and excellent when $1.0 > Z \geq 0.5$. If $0.5 > Z \geq 0.0$, the assay cannot be employed in high-throughput format, and if $Z < 0$, screening is impossible.

SOP for Agar Plate Preparation

Agar plates were prepared by addition of LB medium (250 mL) to 5 g agar. The resulting suspension was stirred and autoclaved. Then, the solution was cooled down to 50 °C while stirring. Afterwards, kanamycin (250 µL, 50 mg/mL) was added to the solution. The solution was shortly stirred and finally added to the petri dishes.

SOP for Colony Growth on Agar Plates for TK_{gst} L382X/D470X Library Screening

To a round bottom microtiter plate, LB medium (130 µL) containing kanamycin (50 mg/mL) was added. The plate was covered with a sealing foil and a hole was perforated in each well for aeration. Meanwhile, the glycerol stocks from the L382X/D470X library plate were thawed at room temperature. The foil was shortly removed and the plate was inoculated with *E. coli* BL21(DE3) cells (5 µL) carrying coding plasmids for the transketolase gene of interest. The plate was sealed again and incubated at 30 °C and 900 rpm for 16–18 hours. When performing assays with BL21 (DE3) untransformed cells or empty plasmid as controls, the inoculation was done from the glycerol stocks with sterilized toothpicks. For the assays with BL21 (DE3) untransformed, no antibiotic was added to the LB medium. After incubation, 20 µL from each well were combined and mixed for the whole library plate screening. Either the cell mixture was then diluted 1 to 10^{-6} with LB medium supplemented with kanamycin (50 mg/mL), or the single clones as in the experiments with untransformed BL21 (DE3) cells or the TK_{gst} N/S variant. The dilutions were vortexed to ensure a good mix and 100 µL were plated out on LB agar plates supplemented with kanamycin (100 µg/mL) as antibiotic. For assays containing untransformed BL21 (DE3) cells, LB plates without antibiotic were used. The plates were incubated at 37 °C for 17–18 h to provide well-dispersed, homogeneous colonies of a reasonable size.

Membrane Transfer, Expression, Masterplate Preparation and Permeabilization

The colonies were first transferred to a labeled nylon Hybond-*N*-membrane by gently pressing the membrane against the agar plate until it was completely adsorbed to the agar. Then the membrane with the colonies stuck to it was taken off from the agar and placed, with the colonies facing up, on an induction plate containing IPTG (2 mM) as inducer and kanamycin (100 µg/mL). Again, for the untransformed BL21 (DE3) colonies the plates were missing the antibiotic. The induction plate carrying the membrane was incubated for 4 to 6 hours at 37 °C. The original agar plate from which the colonies had been removed ("master plate") was incubated again at 37 °C for around 5 h until the colonies had regrown again and thus could be easily picked for sequencing or further rounds of screening. Finally, the master plate was secured with parafilm and stored at 4° C until further use. Cell permeabilization was performed by immersing the membranes in liquid nitrogen for 5 to 10 seconds.

Solid-Phase Supported Assay Procedure

Filter paper was soaked in the reagent's solution containing **1 a** (15 mM), HPA (15 mM), ThDP (0.6 mM), $MgCl_2$ (2.5 mM) and TEA buffer (5 mM, pH 7.45). For the negative controls lacking substrates, the filter paper was soaked only in TEA buffer (5 mM, pH 7.45). Then, the membranes were placed on top of the filter papers, with the colonies facing up, and incubated at 37 °C for 30 minutes. Afterwards, the membranes were dipped 5–10 sec into an aqueous $FeCl_3$ (252 mM) solution for color development. Photos of the colored membranes were immedi-

© 2023 The Authors. Advanced Synthesis & Catalysis published by Wiley-VCH GmbH

ately taken upon ferric chloride staining and computationally flipped to obtain their mirror image for colony picking.

Acknowledgements

This work was supported by The German Federal Ministry of Education and Research (BMBF) under Grant Agreement No 031B0595 ("Tralaminol") within the initiative ERA CoBioTech. The latter has received funding from the European Union's Horizon 2020 Research and Innovation Programme under grant agreement No 722361. Open Access funding enabled and organized by Projekt DEAL

References

[1] G. Schenk, R. G. Duggleby, P. F. Nixon, *Int. J. Biochem. Cell Biol.* **1998**, *30*, 1297–1318.
[2] a) E. Racker, G. De La Haba, I. G. Leder, *J. Am. Chem. Soc.* **1953**, *75*, 1010–1011; b) S. R. Marsden, L. Gjonaj, S. J. Eustace, U. Hanefeld, *ChemCatChem* **2017**, *9*, 1808–1814.
[3] J. Abdoul-Zabar, I. Sorel, V. Helaine, F. Charmantray, T. Devamani, D. Yi, V. de Berardinis, D. Louis, P. Marliere, W.-D. Fessner, L. Hecquet, *Adv. Synth. Catal.* **2013**, *355*, 116–128.
[4] M. Lorilliere, R. Dumoulin, M. L'enfant, A. Rambourdin, V. Thery, L. Nauton, W.-D. Fessner, F. Charmantray, L. Hecquet, *ACS Catal.* **2019**, *9*, 4754–4763.
[5] J. Abdoul-Zabar, M. Lorilliere, D. Yi, T. Saravanan, T. Devamani, L. Nauton, F. Charmantray, V. Helaine, W.-D. Fessner, L. Hecquet, *Adv. Synth. Catal.* **2015**, *357*, 1715–1720.
[6] D. Yi, T. Saravanan, T. Devamani, F. Charmantray, L. Hecquet, W.-D. Fessner, *Chem. Commun.* **2015**, *51*, 480–483.
[7] T. Saravanan, M.-L. Reif, D. Yi, M. Lorillière, F. Charmantray, L. Hecquet, W.-D. Fessner, *Green Chem.* **2017**, *19*, 481.
[8] C. Zhou, T. Saravanan, M. Lorilliere, D. Wei, F. Charmantray, L. Hecquet, W.-D. Fessner, D. Yi, *ChemBioChem* **2017**, *18*, 455–459.
[9] a) T. Saravanan, S. Junker, M. Kickstein, S. Hein, M.-K. Link, J. Ranglack, S. Witt, M. Lorilliere, L. Hecquet, W.-D. Fessner, *Angew. Chem. Int. Ed.* **2017**, *56*, 5358–5362; b) H. Casajus, L. Nauton, A. Lagarde, V. Thery, F. Charmantray, M. Leremboure, W.-D. Fessner, L. Hecquet, *ChemCatChem* **2020**, *12*, 5772–5779.
[10] J. L. Galman, D. Steadman, S. Bacon, P. Morris, M. E. B. Smith, J. M. Ward, P. A. Dalby, H. C. Hailes, *Chem. Commun.* **2010**, *46*, 7608–7610.
[11] a) P. Payongsri, D. Steadman, J. Strafford, A. MacMurray, H. C. Hailes, P. A. Dalby, *Org. Biomol. Chem.* **2012**, *10*, 9021–9029; b) P. Payongsri, D. Steadman, H. C. Hailes, P. A. Dalby, *Enzyme Microb. Technol.* **2015**, *71*, 45–52; c) P. E. Affaticati, S.-B. Dai, P. Payongsri, H. C. Hailes, K. Tittmann, P. A. Dalby, *Sci. Rep.* **2016**, *6*, 35716; d) H. Yu, R. I. H. Lopez, D. Steadman, D. Mendez-Sanchez, S. Higson, A. Cazares-Korner, T. D. Sheppard, J. M. Ward, H. C. Hailes, P. A. Dalby, *FEBS J.* **2020**, *287*, 1758–1776; e) H. C. Wilkinson, P. A. Dalby, *FEBS J.* **2021**, *288*, 1935–1955.
[12] I. Fúster Fernández, L. Hecquet, W.-D. Fessner, *Adv. Synth. Catal.* **2022**, *364*, 612–621.
[13] Y. V. Sheludko, W.-D. Fessner, *Curr. Opin. Struct. Biol.* **2020**, *63*, 123–133.
[14] a) D. Yi, T. Devamani, J. Abdoul-Zabar, F. Charmantray, V. Helaine, L. Hecquet, W.-D. Fessner, *ChemBioChem* **2012**, *13*, 2290–2300; b) G. Simon, T. Eljezi, B. Legeret, F. Charmantray, J. Castillo, C. Guerard-Helaine, M. Lemaire, M. Bouzon-Bloch, P. Marliere, V. Helaine, L. Hecquet, *ChemCatChem* **2013**, *5*, 784–795; c) L. Hecquet, W.-D. Fessner, V. Helaine, F. Charmantray, in *Cascade Biocatalysis: Integrating Stereoselective and Environmentally Friendly Reactions* (Eds.: S. Riva, W.-D. Fessner), Wiley-VCH, Weinheim, **2014**, pp. 315–337.
[15] A. Ranoux, S. K. Karmee, J. Jin, A. Bhaduri, A. Caiazzo, I. W. C. E. Arends, U. Hanefeld, *ChemBioChem* **2012**, *13*, 1921–1931.
[16] M. E. B. Smith, U. Kaulmann, J. M. Ward, H. C. Hailes, *Bioorg. Med. Chem.* **2006**, *14*, 7062–7065.
[17] N. Ocal, A. Lagarde, L. Hecquet, *ChemBioChem* **2021**, *22*, 11–18.
[18] J. B. Neilands, *Science* **1967**, *156*, 1443–1447.
[19] U. Nilsson, L. Hecquet, T. Gefflaut, C. Guerard, G. Schneider, *FEBS Lett.* **1998**, *424*, 49–52.
[20] a) O. N. Solovjeva, M. V. Kovina, M. G. Zavialova, V. G. Zgoda, D. S. Shcherbinin, G. A. Kochetov, *Biosci. Rep.* **2020**, *40*, BSR20180246; b) O. N. Solovjeva, *Anal. Biochem.* **2021**, *613*, 1–14.
[21] W. L. DeLano, *The PyMOL Molecular Graphics System*, Version 1.3 **2002**, Schrödinger LLC, http://www.pymol.org.
[22] U. Nilsson, L. Meshalkina, Y. Lindqvist, G. Schneider, *J. Biol. Chem.* **1997**, *272*, 1864–1869.
[23] a) H. Xiao, Z. Bao, H. Zhao, *Ind. Eng. Chem. Res.* **2015**, *54*, 4011–4020; b) S. R. Nirantar, *Molecules* **2021**, *26*, 5599.
[24] H. Leemhuis, R. M. Kelly, L. Dijkhuizen, *IUBMB Life* **2009**, *61*, 222–228.
[25] M. S. Packer, D. R. Liu, *Nat. Rev. Genet.* **2015**, *16*, 379–394.
[26] M. S. Weiß, I. V. Pavlidis, C. Vickers, M. Höhne, U. T. Bornscheuer, *Anal. Chem.* **2014**, *86*, 11847–11853.
[27] T. Yoshioka, T. Uematsu, *Drug Metab. Dispos.* **1998**, *26*, 705–710.
[28] F. Dickens, D. H. Williamson, *Biochem. J.* **1958**, *68*, 74–81.

© 2023 The Authors. Advanced Synthesis & Catalysis published by Wiley-VCH GmbH